Oscillation quenching and phase-flip bifurcation in coupled thermoacoustic systems

Suraj Dange (iD), Krishna Manoj (iD), Subham Banerjee (iD), Samadhan A. Pawar (iD), Sirshendu Mondal (iD), and R. I. Sujith (iD)

View Online   Export Citation   CrossMark

ARTICLES YOU MAY BE INTERESTED IN

Oscillation quenching and phase-flip bifurcation in coupled thermoacoustic systems

Suraj Dange,[1] 🆔 Krishna Manoj,[1,a)] 🆔 Subham Banerjee,[1] 🆔 Samadhan A. Pawar,[1] 🆔 Sirshendu Mondal,[2] 🆔 and R. I. Sujith[1] 🆔

AFFILIATIONS

[1] Department of Aerospace Engineering, Indian Institute of Technology Madras, Chennai 600036, India
[2] Department of Mechanical Engineering, National Institute of Technology Durgapur, Durgapur 713209, India

[a)] Electronic mail: krishnanalinam@gmail.com

ABSTRACT

Oscillatory instabilities, although ubiquitous in nature, are undesirable in many situations such as biological systems, swaying of bridges and skyscrapers, aero-acoustic flutter, prey-predator and disease spread models, and thermoacoustic systems, where they exhibit large amplitude periodic oscillations. In the present study, we aim to study the suppression mechanism of such undesired oscillations in a pair of thermoacoustic oscillators, also known as horizontal Rijke tubes. These oscillators are coupled through a connecting tube whose length and diameter are varied as coupling parameters. With the variation of these parameters, we show the first experimental evidence of rich dynamical phenomena such as synchronization, amplitude death, and phase-flip bifurcation in coupled identical thermoacoustic oscillators. We discover that when frequency and amplitude mismatch are introduced between these oscillators, quenching of oscillations in one or both the oscillators occurs with further ease, through the mechanisms of amplitude death and partial amplitude death. Finally, we show that the effectiveness of coupling is sensitive to the dimensions of the connecting tube which can be directly correlated with the time delay and coupling strength of the system.

Published under license by AIP Publishing. https://doi.org/10.1063/1.5114695

The occurrence of undesirable large amplitude, self-sustained periodic acoustic oscillations observed in confined combustion systems is referred to as thermoacoustic instability. Mitigation of such instabilities remains a challenge, even after decades of extensive research. In the current study, we use concepts from synchronization theory to mitigate thermoacoustic instability. Toward this, we couple two horizontal Rijke tubes in the thermoacoustic instability state of operation, using a connecting tube whose dimensions are varied as the control parameters. The variation of the length of the connecting tube leads to the transition from antiphase to in-phase synchronization via the state of amplitude death, i.e., the complete quenching of oscillations in both the systems, for low amplitude limit cycle oscillations in identical thermoacoustic systems. On the other hand, an abrupt transition from antiphase to in-phase synchronization, commonly referred to as phase-flip bifurcation, is observed in the case of high amplitude limit cycle oscillations in such systems. Therefore, any combination of length and diameter of the connecting tube proves insufficient in suppressing high amplitude oscillations in identical Rijke tube oscillators. In order to obtain complete mitigation of such high amplitude oscillations, we introduce frequency detuning

between the oscillators. As the detuning between the oscillators is gradually increased, we notice an increase in the suppression of amplitudes of oscillations in both the oscillators, leading to the phenomenon of amplitude death. A further increase in the frequency detuning leads to the occurrence of partial amplitude death in the system, where the oscillations in one oscillator are nearly quenched while they are sustained in the other. We further investigate the regimes of amplitude suppression in the system for the combined addition of frequency detuning and amplitude mismatch between the oscillators. We observe enhanced suppression of oscillations in the system due to the addition of mismatch in system parameters.

I. INTRODUCTION

Oscillatory motions arising in natural systems can either be desirable or undesirable based on our perspective. Oscillations in a pendulum clock,[1] breathing patterns in animal species,[2] and oscillations produced in musical instruments[3] are a few examples of oscillations that are considered desirable. However, oscillations in cases

such as ecological systems, such as prey-predator systems,[4] epidemic spread systems,[5] precision instrument manufacturing,[6] lasers,[7] and structural systems,[8,9] and biological systems, such as neuro-muscular systems,[10] are undesirable. The uncontrolled amplification of such undesirable oscillations beyond a critical threshold can lead to catastrophic disasters. Some noteworthy examples of such catastrophes are the collapse of the Tacoma Bridge,[11] swaying of the Millennium Bridge[12] leading to its shut down, or thermoacoustic instability leading to failure of rockets and gas turbine engines.[13]

One of the well-studied cases of such undesirable oscillations which hindered the development of gas turbine industry, rocket engines, and power generation units is the issue of thermoacoustic instability.[14,15] Thermoacoustic instability refers to the occurrence of high amplitude acoustic pressure oscillations inside a combustor due to the positive feedback between the acoustic field of the combustor and the heat release rate fluctuations in the flame.[14,15] The presence of such instabilities has led to various damages ranging from the destruction of gas turbine engine components during testing to massive structural damage in the Rocketdyne F-1 rocket engine in Saturn V program.[16] Several control strategies such as active and passive controls have been developed over the years to suppress thermoacoustic instability by disrupting the coupling between the acoustic field and the unsteady flame dynamics and increasing the acoustic damping of the system, respectively.[17–19] Although these strategies prove very effective, they often face problems related to installations of actuators/sensors amidst harsh conditions as well as their limited applicability due to the restricted operational range. Apart from these techniques of suppressing such oscillations, recent studies focus on the application of synchronization theory[20,21] in suppressing the oscillations in one[22,23] or multiple thermoacoustic systems.[24–26]

Synchronization is a universal phenomenon marked by the adjustment of rhythm of coupled oscillators due to mutual interaction between them.[20] Such mutual coupling between two self-sustained nonlinear oscillators can exhibit various phenomena such as phase-locking, phase-drifting, phase-flip bifurcation, and oscillation quenching.[27] In the case of weakly coupled oscillators, the mutual interaction between the oscillators is limited to their phases; hence, they exhibit phase-locking behavior or synchronization. On the other hand, strong mutual coupling affects both the phase and the amplitude of coupled oscillations, causing the reduction or complete cessation of oscillations in all the oscillators. Such a dynamical behavior wherein all the oscillators approach a common steady state due to coupling is referred to as amplitude death and was discovered by Strutt and Rayleigh[28] in a system of two organ pipes. In some situations, mutual coupling does not necessarily lead to quenching of oscillations in all the coupled oscillators; it may result in a coexistence of oscillatory and steady states, which is referred to as partial amplitude death (PAD).[29]
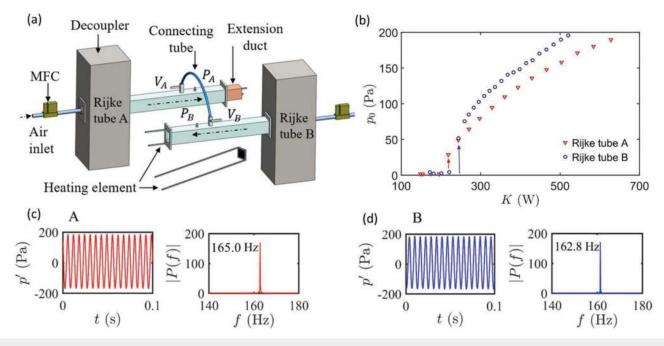
The occurrence of the oscillation quenched states due to the coupling of two or more oscillators in thermoacoustic systems has lured recent research attention. The experimental study by Biwa et al.[24] showed the occurrence of amplitude death in two thermoacoustic engines for simultaneous application of dissipative and time delay couplings, even for zero frequency detuning. In a thermoacoustic engine, the conversion of thermal power into acoustic power results in high amplitude pressure oscillations.[30] A thermoacoustic engine consists of a porous stack placed between hot and cold

exchangers in a tube, and the temperature difference across the stack amplifies the acoustic fluctuations. On the other hand, the feedback between the acoustic field and the unsteady flame dynamics in the presence of a mean flow in a confinement results in thermoacoustic instability. A recent study by Thomas et al.[25] systematically investigated the amplitude death phenomenon in a mathematical model of coupled horizontal Rijke tube oscillators, when both dissipative and time delay coupling are applied collectively and individually. They further extended the study[31] to characterize the effect of Gaussian white noise on the amplitude death behavior of such coupled oscillator systems. They noticed prebifurcation noise amplification during the transition from limit cycle to amplitude death state, and vice versa.

An experimental study by Hyodo and Biwa[32] compared the effect of connecting two thermoacoustic engines with single and two connecting tubes on their amplitude death behavior. They found that a single tube, having a diameter of 62.5% of the resonance tube, is as effective as two connecting tubes, having a diameter of 7.5% of the resonance tube, in suppressing the oscillations. A recent study by Jegal et al.[26] investigated the amplitude death behavior in two turbulent thermoacoustic combustors connected through a cross talk arrangement. They observed that the combustors operating under stable conditions were excited to high amplitude oscillations after being coupled via the cross talk. They also observed amplitude death after coupling the oscillators, having asymmetric boundary conditions, in their unstable state. Although the aforementioned studies provide a cognizance on the oscillation quenching mechanism in coupled thermoacoustic oscillators, a systematic experimental investigation to understand the role of connecting tube dimensions (i.e., length and diameter) and parameter mismatch, such as amplitude and frequency of limit cycle oscillators, on their quenching behavior is yet to be reported.

II. EXPERIMENTAL SETUP AND DATA ANALYSIS

The experimental setup [Fig. 1(a)] used to study the amplitude quenching behavior of limit cycle oscillations (LCOs) consists of a pair of horizontal Rijke tubes (named as A and B). In these systems, an electrically heated wire mesh acts as the heating source.[33] The detailed characteristics of a single horizontal Rijke tube system can be obtained from Matveev[33] and Gopalakrishnan and Sujith.[34] Here, Rijke tube A [Fig. 1(a)] has a cross section of $9.3 \times 9.4 \, \text{cm}^2$ and is 102.0 cm long, while Rijke tube B has a cross section of $9.3 \times 9.5 \, \text{cm}^2$ and a length of 104.0 cm. Separate decouplers of dimensions $120.0 \times 45.0 \times 45.0 \, \text{cm}^3$ are attached to the inlet of both the Rijke tubes to ensure that the flow entering the systems is immune from the upstream disturbances. The dimensions of the decoupler being much bigger than the cross section of the duct, the pressure is maintained at ambient conditions (acoustic pressure fluctuations, $p' = 0 \, \text{Pa}$) at both ends. Separate heating elements are located at a distance of 27.5 cm from the decoupler in each system. A mean air flow rate of 40 SLPM (standard liter per minute) is supplied to each system through separate mass flow controllers (Alicat Scientific, with an uncertainty of ± 0.52 SLPM). The decay rates of each system are experimentally measured in the absence of flow by subjecting the systems to external sinusoidal perturbations using a loudspeaker (Ahuja AU60). The acoustic decay rate values for Rijke tube A and Rijke tube

FIG. 1. (a) Schematic of the experimental setup having two horizontal Rijke tube oscillators A and B, which are coupled using a connecting tube. (b) Variation of root mean square amplitude, p_0, with heater power (K) for the isolated Rijke tube oscillators A (red triangles) and B (blue circles). (c) and (d) The time series of limit cycle oscillations and the corresponding amplitude spectrum of Rijke tube oscillators A and B, respectively, prior to coupling. The uncoupled natural frequency of oscillator A is $f_{0A} = 165.0 \pm 1.1$ Hz and oscillator B is $f_{0B} = 162.8 \pm 1.1$ Hz.

B are measured to be $14.5 \pm 0.5 \, \mathrm{s}^{-1}$ and $12.7 \pm 0.6 \, \mathrm{s}^{-1}$, respectively. We maintain the acoustic decay rate within bounds to ensure consistency in the experimental conditions and the repeatability of the experimental results.

The characterization of the individual Rijke tube oscillators is performed by analyzing their amplitude and frequency response with a change in the heater power (K). Figure 1(b) shows the variation of root mean square value, henceforth referred to as amplitude, of acoustic pressure oscillations (p_0) of the uncoupled oscillators A and B with the heater power (K). We observe that both the systems exhibit Hopf bifurcation, i.e., the transition from a steady state to stable limit cycle oscillations [shown in Figs. 1(c) and 1(d)], at different critical values of K, owing to the difference in decay rates of each oscillator. We also observe a small difference in the frequency of oscillator A (165.0 Hz) and B (162.8 Hz) due to the difference in their lengths. In order to study the dynamics of identical oscillators, the amplitude and frequency of oscillator A are adjusted by varying the heater power and the length of the oscillator, respectively, such that the resultant uncoupled amplitude and frequency values of oscillator A are equal to that of oscillator B.

The position of a square extension duct of side 9.0 cm and length 12.0 cm is manually changed to vary the natural frequency of Rijke tube A initially from 165.0 Hz to 162.8 Hz to make both Rijke tube oscillators identical. Although, identical conditions cannot be attained in practice and the oscillators are only nearly identical, the uncertainty being small, we refer to these oscillators having nearly equal amplitude and frequency as identical in Secs. III A–III C. The

limit cycle dynamics of these systems are coupled by connecting them using a vinyl tube, whose length and diameter are varied as control parameters [see Fig. 1(a)]. The length (L') of the connecting tube is varied from 72.0 cm to 132.0 cm in steps of 5.0 cm, while the diameter (D) is varied from 0.4 cm to 1.2 cm in steps of 0.2 cm. Here, the length of the connecting tube (L') is normalized with the wavelength ($L = L'/\lambda$, where $\lambda = c/f_{0B}$ and c is the speed of sound at ambient conditions) of acoustic standing wave developed in oscillator B (the oscillator whose length remains constant throughout the study). The coupling ports for the vinyl tube, indicated as V_A and V_B, are located at a distance of 46.5 cm from the outlet of both the Rijke tubes and are equipped with ball-type valves, which are manually opened to initiate the coupling between the systems.

Simultaneous measurements of acoustic pressure fluctuations are performed prior to and after the initiation of coupling using pressure transducers (PCB 103B02, with an uncertainty of ± 0.2 Pa) located at positions P_A and P_B, at a distance of 31.5 cm from the outlet of the tubes, as shown in Fig. 1(a). The data are acquired from each oscillator at a sampling rate of 10 kHz for a duration of 25 s for each set of experiments using a DAQ system (NI USB 6343). All experiments conducted to study the synchronization and the suppression of oscillation after coupling are carried out at values sufficiently away from the Hopf point of both the oscillators.

Further analysis on the coupled dynamics of these oscillators is performed after an introduction of frequency and amplitude mismatch in the system. The amplitude mismatch (Δp_0) and frequency detuning (Δf) in the system are defined as $\Delta p_0 = |p_{0A} - p_{0B}|$ and

$\Delta f = |f_{0A} - f_{0B}|$, where $\{p_{0A}, f_{0A}\}$ and $\{p_{0B}, f_{0B}\}$ are the amplitudes and frequency of oscillators A and B, respectively, in their uncoupled state. Since the frequency of acoustic oscillations in the duct is directly dependent on its length, the frequency of oscillator A is varied from 147.8 Hz to 162.8 Hz by varying its effective length using an extension duct. This frequency variation in oscillator A corresponds to 0–15.0 Hz of frequency detuning in the system. The frequency of limit cycle oscillations in oscillator B (f_{0B}) is maintained constant throughout the study. The normalized frequency detuning ($\Delta f / f_{0B}$) corresponding to this frequency change in oscillator A with respect to oscillator B is nearly 0–0.092. Similarly, the amplitude mismatch between the acoustic oscillations in both the oscillators is introduced by varying the heater power (K) of oscillator A with respect to that of oscillator B.

III. RESULTS

Here, we present the results obtained by varying the coupling and the system parameters, and present their effects on the amplitude suppression behavior of the coupled Rijke tube oscillators. The study is conducted for the variation of four independent parameters, which are (1) length (L) and (2) diameter (D) of the connecting tube, and (3) frequency detuning (Δf), and (4) amplitude mismatch (Δp_0) of the limit cycle oscillations in the system. The results obtained from each of these cases are individually presented in Secs. III A–III C.

A. Effect of variation in coupling parameters on identical oscillators

The primary methodology adopted to quench thermoacoustic oscillations in identical Rijke tube systems is to vary the length (L) of the connecting tube having a diameter of 1.0 cm. Toward this purpose, the amplitude and frequency in the uncoupled state of the

Rijke tube oscillators A and B are maintained at nearly equal values, and the acoustic responses of the systems are measured for each length (L) of the connecting tube. The synchronization analysis of the acoustic pressure data is performed by extracting the instantaneous phases of both the oscillators using the Hilbert transform,[20] which helps in extending the signal from the real plane to a complex plane. Hence, we obtain the analytic signal, $\zeta(t) = p(t) + p_H(t)$, where $p(t)$ is the acquired pressure signal and $p_H(t)$ is its corresponding Hilbert transformed signal given by
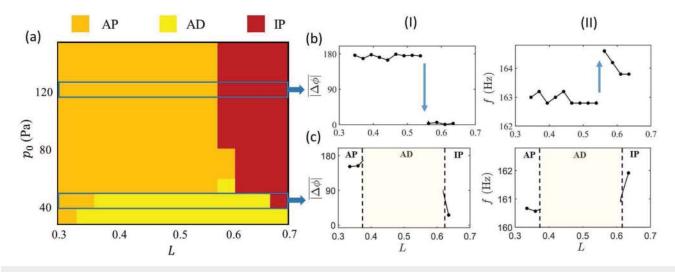
$$p_H(t) = \frac{1}{\pi} P.V. \int_{-\infty}^{\infty} \frac{p(\tau)}{t - \tau} d\tau, \qquad (1)$$

where $P.V.$ is the Cauchy Principle value. The instantaneous phases of each signal, $\Phi(t)$, are obtained from the analytic signal as $\zeta(t) = A(t) \exp(i\Phi(t))$. The relative phase between the signals of oscillators A and B is obtained from the difference of their instantaneous phases [$\Phi_A(t)$ and $\Phi_B(t)$, respectively] as $\Delta\Phi(t) = \Phi_A(t) - \Phi_B(t)$. When the coupled oscillators are synchronized, the temporal variation of relative phase between them fluctuates around a constant value. This constant value of relative phase is computed in terms of mean phase difference between the two signals ($\overline{|\Delta\Phi|}$) as follows:

$$\overline{|\Delta\Phi|} = \frac{1}{N} \Sigma_{t=1}^{N} |\Delta\Phi(t)|, \qquad (2)$$

where N is the total number of samples in the signal and $\Delta\Phi(t)$ is the instantaneous phase difference (wrapped in the interval of $0°$ and $180°$) between two oscillators.

Figure 2(a) shows the two-parameter bifurcation plot between the uncoupled amplitude (p_0) of the oscillators and the length (L) of the connecting tube used for coupling the identical oscillators. We observe that for lower values of p_0, the coupled dynamics exhibited by the system transition from a state of antiphase synchronization to in-phase synchronization via an intermediate state of amplitude

FIG. 2. (a) Two-parameter bifurcation plot between the uncoupled amplitude of pressure oscillation (p_0) and the length (L) of the connecting tube, displaying the coexistence of amplitude death and phase-flip bifurcation in a system of identical oscillators. Depending on the value of the uncoupled amplitude of the oscillators, the coupled dynamics of the system exhibits either (b) phase-flip bifurcation for higher values or (c) transition from anti-phase (AP) to in-phase synchronization (IP) via amplitude death (AD) for lower values.
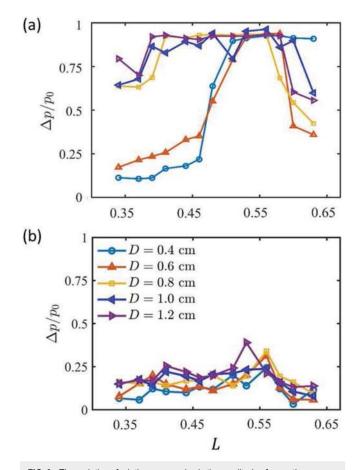
death (AD) as L is increased [as shown in Fig. 2(c)]. The state of antiphase synchronization is characterized by a phase shift of nearly 180° between the oscillators, whereas, during the state of in-phase synchronization, both oscillators exhibit nearly 0° of phase shift. The dominant frequency of the oscillators is observed to be lower during antiphase synchronization and higher during in-phase synchronization, as compared to their uncoupled value. In the intermediate state between antiphase and in-phase synchronization, we observe complete quenching of oscillations in both the oscillators due to coupling, and thus, the system behavior converges to a homogeneous steady state. Such a state of coupled dynamics is termed as amplitude death.[35] The instantaneous phase calculated using the Hilbert transform is undefined due to the lack of oscillations during this state and hence is not discussed in Fig. 2(c).

When the amplitude of acoustic pressure oscillations in the uncoupled state of the oscillators is sufficiently high, we observe an abrupt transition from antiphase synchronization to in-phase synchronization, as the length of the connecting tube is increased [see Fig. 2(b)]. During this transition, the mean value of the phase difference between the oscillators abruptly changes from nearly 180° to 0° [Fig. 2(b)-I], which is accompanied by a corresponding jump in their dominant frequency [Fig. 2(b)-II]. Such a sudden switching of phase difference between the oscillators at a critical value of the coupling parameter is commonly referred to as phase-flip bifurcation, PFB.[36] The direction of jump in the frequencies of oscillators during the PFB observed in our system is opposite to what is usually reported in the literature,[36,37] where such a synchronization transition is associated with a decrease in the frequency of oscillators. From Fig. 2(b), we observe that the critical value of L at which the PFB happens is around 0.53. Previous theoretical studies by Thomas *et al.*[25,31] on similar Rijke tube oscillators have reported the existence of AD in identical oscillators. They showed that, when the oscillators are only time delay coupled, the increase in amplitude of limit cycle oscillations reduces the region for which AD is observed in the parameter space of coupling constants (i.e., delay and coupling strength) in the system. However, their study did not report the existence of PFB in the model of coupled Rijke tube oscillators. We here, report the first experimental evidence of phase-flip bifurcation in coupled thermoacoustic systems. We also conclude that a connecting tube of appropriate length [in the range shown in Fig. 2(a)] is sufficient to quench the undesired thermoacoustic oscillations with low amplitude and is insufficient to do so for the high amplitude oscillations in coupled Rijke tube oscillators.

Now, let us take a closer look at the suppression behavior of acoustic oscillations in coupled identical Rijke tubes when the amplitude of their oscillations in the uncoupled state is low ($p_0 = 40$ Pa) and high ($p_0 = 120$ Pa). We study this behavior of oscillators when the dimensions (L and D) of the connecting tube are varied. Here, the suppression in the amplitude is quantified as $\Delta p = p_0 - p$, where p_0 and p are the amplitudes of acoustic pressure oscillations before and after the initiation of coupling, respectively. The suppression is normalized with the uncoupled amplitude (p_0) such that $\Delta p/p_0 = 1$ corresponds to complete suppression (or amplitude death) and $\Delta p/p_0 = 0$ points toward the lack of suppression in the amplitudes of Rijke tube oscillators.

When the amplitude of pressure oscillations is low ($p_0 = 40$ Pa), we observe that the relative suppression of coupled oscillations varies

significantly with the diameter of the connecting tube [Fig. 3(a)]. For smaller diameters of the connecting tube ($D = 0.4$ cm and 0.6 cm), we observe the presence of weak coupling between the oscillators A and B when $L < 0.48$, which in turn, is projected as the lack of suppression in the oscillations in Fig. 3(a). In contrast, we observe a complete suppression in oscillations for $L \geq 0.48$ until the system dynamics transition to in-phase synchronization at $L = 0.58$. Such an interaction among the oscillators leading to changes in the amplitude of coupled oscillations for $L \geq 0.48$ suggests the existence of stronger coupling between them. When the diameter of the connecting tube is larger, $D \geq 0.8$ cm, we observe an increase in the suppression of acoustic pressure oscillations in coupled Rijke tubes, in the entire range of L considered in our study. Furthermore, the system dynamics exhibits the state of amplitude death ($\Delta p/p_0 \to 1$) for L ranging from 0.39 to 0.58, irrespective of the value of D used for the connecting tube. These observations further suggest that the occurrence of AD is possible only for certain combinations of dimensions (L and

FIG. 3. The variation of relative suppression in the amplitude of acoustic pressure oscillations ($\Delta p/p_0$) in oscillator A is plotted with respect to the length of the connecting tube (L), for various values of diameter (D). The amplitude of uncoupled oscillations, p_0, is 40 Pa in (a) and 120 Pa in (b). A similar trend can be observed in the case of oscillator B.

D) of the connecting tube when low amplitude identical Rijke tube oscillators are coupled.

For the case shown in Fig. 3(b) with $p_0 = 120$ Pa, we see that the variation in the relative suppression ($\Delta p/p_0$) of acoustic pressure oscillations with the length of the connecting tube remains nearly the same, irrespective of the diameter of the connecting tube used. Hence, we can conclude that any combination of length and diameter of the connecting tube considered in the current study proves ineffective in suppressing high amplitude pressure oscillations of identical Rijke tube oscillators.

B. Effect of frequency detuning on the amplitude suppression behavior of coupled oscillators

Having discussed the insufficiency of variation in the dimensions (i.e., length and diameter) of the connecting tube in complete suppression of high amplitude acoustic pressure oscillations ($p_0 > 60$ Pa), we introduce frequency detuning in the system to suppress them. The amplitudes of limit cycle oscillations in the uncoupled state, p_0, of both the oscillators are kept nearly constant at 120 Pa. The dimensions of the connecting tube ($L = 0.48$ and $D = 1.0$ cm) are fixed such that they correspond to the maximum suppression of limit cycle oscillations after coupling [as observed in Figs. 3(a) and 3(b)]. The introduction of frequency detuning in coupled Rijke tubes engendered an increase in the suppression of pressure oscillations in both the systems [Fig. 4(a)]. For low values of detuning (say,

0–4.0 Hz), we observe that the suppression in the amplitude of coupled oscillations increases monotonically with detuning. We observe nearly 10% reduction in the amplitude of limit cycle oscillations in both the Rijke tubes for $\Delta f = 0$ Hz [Fig. 4(c)], which increases to nearly 60% for $\Delta f = 4.0$ Hz [Fig. 4(d)]. In addition to the reduction in amplitude, we also note that coupling these detuned oscillators causes mutual synchronization between them, leading both the oscillators to stabilize at identical frequencies [as shown in Fig. 4(b)]. With a further increase in the value of frequency detuning, 4.0 Hz $< \Delta f < 9.0$ Hz, we observe complete quenching of pressure oscillations (i.e., $\Delta p/p_0 \approx 1$) in both the systems, which is also referred to as the state of amplitude death. Figure 4(e) represents such a case of amplitude death, with simultaneous quenching of oscillations in both the oscillators, leading to the absence of periodic behavior in their dynamics, for $\Delta f = 7.0$ Hz.

When the frequency detuning in the system is sufficiently large, $\Delta f >= 9.0$ Hz, we observe that one among the oscillators regains its periodic oscillations while the other oscillator remains in a nearly quenched state. Such a phenomenon of oscillation quenching, where limit cycle oscillations of one oscillator coexists with a nearly quenched state of another due to coupling, is referred to as partial amplitude death.[29,38] For the frequency detuning of $\Delta f = 15.0$ Hz, we notice that the oscillations in Rijke tube B are nearly quenched (i.e., minimal fluctuations) while that in Rijke tube A retain the state of large amplitude limit cycle oscillations [see Fig. 4(f)]. We also note that during the state of partial amplitude death, both the oscillators
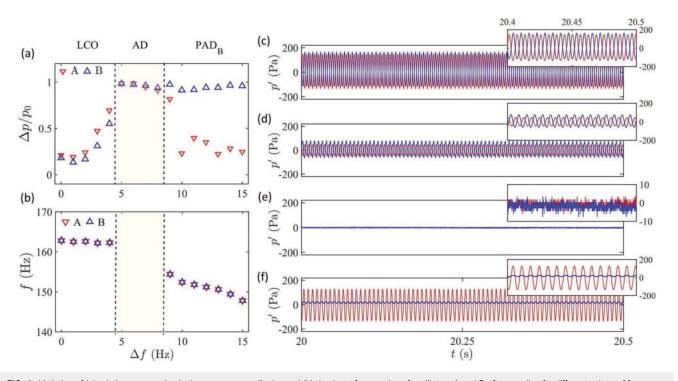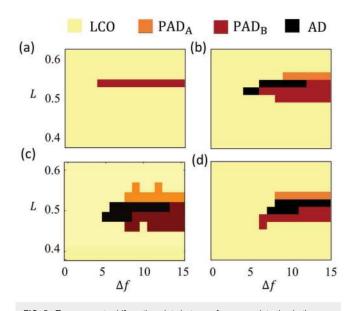

FIG. 4. Variation of (a) relative suppression in the response amplitudes and (b) dominant frequencies of oscillators A and B after coupling for different values of frequency detuning, Δf, when $L = 0.48$, $D = 1.0$ cm, and $p_0 = 120$ Pa. The time series corresponding to various states of coupled dynamics observed for frequency detuning of (c) 0 Hz—no suppression, (d) 4.0 Hz—significant suppression, (e) 7.0 Hz—amplitude death, and (f) 15.0 Hz—partial amplitude death.

exhibit identical frequencies [see Fig. 4(b)], whose value tends to be closer to that of the oscillator with higher amplitude. In other words, in Fig. 4(f), where oscillator A exhibits higher amplitude oscillations compared to oscillator B, both the oscillators oscillate with a frequency near the uncoupled frequency value of oscillator A [see Fig. 4(b)]. This also suggests that the oscillator which regains its oscillations during the state of partial amplitude death drives the oscillations in the other oscillator which is oscillating at significantly lower amplitudes.

In Fig. 5, we show the coupled dynamics of limit cycle oscillations (LCO) developed in detuned Rijke tube oscillators for various dimensions (L and D) of the connecting tube. The amplitudes of both LCO are fixed at 120 Pa in their uncoupled state. Two-parameter bifurcation plots between the length of the connecting tube (L) and the frequency detuning between oscillators (Δf) are plotted for various values of connecting tube diameters (D). For a lower value of the tube diameter, $D = 0.6$ cm [Fig. 5(a)], we notice the existence of only LCO and PAD dynamics for the range of L and Δf investigated in this study. The coupling induced by smaller diameter tube being weak, is insufficient to simultaneously quench the oscillations in both the oscillators. The effect of finite detuning ($\Delta f > 3.0$ Hz) for $L = 0.56$ is noticed only in oscillator B, where the LCO is quenched while they are retained in oscillator A, indicated as PAD$_B$ in Fig. 5(a). On the other hand, when the tube diameter is sufficiently large, $D = 0.8$, 1.0, and 1.2 cm, we see the existence of all LCO, AD, and PAD states in the coupled dynamics of both the Rijke tubes [see Figs. 5(b)–5(d)]. For lower values of frequency detuning ($\Delta f < 4.0$ Hz), we observe LCO in both the oscillators, irrespective of the value of L for all these diameters. When the frequency detuning is relatively high ($\Delta f > 5.0$ Hz), oscillation quenching is observed for a specific range of L in either one or both the Rijke tube oscillators, depending on the dimensions of the tube as is explained subsequently.

For the case of $D = 0.8$ cm, shown in Fig. 5(b), we observe that the AD region is limited to $L \approx 0.5$ at $\Delta f = 3.0$–10.0 Hz. For larger values of detuning ($\Delta f = 8.0$–13.0 Hz), we observe the occurrence of PAD along with the states of LCO and AD in our system. Here, the oscillation quenching states (PAD and AD) are limited over the range of L from 0.46 to 0.55. At very high values of frequency detuning ($\Delta f > 13.0$ Hz), the occurrence of PAD states alone is witnessed for this range of L in the system. A similar scenario is observed in the case of $D = 1.0$ cm as shown in Fig. 5(c); however, we observe that the overall zone of suppression (region covered by AD and PAD states) is increased. For larger values of diameter, $D = 1.2$ cm [see Fig. 5(d)], the value of Δf corresponding to the occurrence of PAD is lower than that corresponding to the state of AD. Further, we observe that for Δf ranging from 6.0 to 15.0 Hz, we observe the existence of AD, PAD and LCO for varying values of L. This is in contrast with the behavior shown by smaller diameters such as 0.8 and 1.0 cm, where we observe the state of PAD and LCO alone at frequency detuning values of $\Delta f > 13.0$ Hz [Figs. 5(b) and 5(c)]. Thus, we can conclude that the amplitude suppression zone of LCOs in coupled Rijke tubes is increased due to the addition of frequency mismatch between the systems, and the suppression is maximum for a finite range of L around 0.5 and $D = 1.0$ cm.

C. Effect of amplitude and frequency mismatch on the amplitude suppression behavior of the coupled oscillators

As we know, the dynamics of most real-world systems with multiple combustors are usually nonidentical. They tend to possess inherent detuning along with a mismatch in the amplitudes of their oscillatory dynamics. Hence, in order to understand the effect of such a mismatch in the system parameters on the suppression of their coupled dynamics, we investigate the coupled behavior of Rijke tube oscillators having a combination of frequency detuning and amplitude mismatch. Toward this purpose, the amplitude of oscillator A in the uncoupled state is varied from 60 to 120 Pa in steps of 10 Pa, through the adjustment of its supplied heater power (K), and the frequency is varied from 162.8 Hz to 147.8 Hz in steps of 1.0 Hz by varying its effective length. On the other hand, the amplitude and frequency of oscillator B are kept constant at 120 Pa and 162.8 Hz, thereby introducing a mismatch in the uncoupled amplitude and frequency values of both the oscillators.

Figures 6(a) and 6(b) show the two-parameter bifurcation plots, highlighting the amplitude suppression (Δp) behavior of LCOs in coupled Rijke tube oscillators A and B, respectively, upon coupling with a single connecting tube. Here, Δp is the difference in the amplitudes of LCO in an oscillator before and after the application of coupling, $p_0 - p$. In Fig. 6, the complete suppression of oscillations is indicated by $\Delta p \approx 120$ Pa (dark zones) and the absence of amplitude suppression after coupling by $\Delta p \approx 0$ Pa (light zones). The existence of $\Delta p \approx 0$ Pa in Figs. 6(a) and 6(b) at identical values of system

FIG. 5. Two-parameter bifurcation plots between frequency detuning in the system (Δf) and length of the connecting tube (L) for diameter values of (a) 0.6 cm, (b) 0.8 cm, (c) 1.0 cm, and (d) 1.2 cm when p_0 is fixed at 120 Pa in both the oscillators. Various states of coupled dynamics, namely, limit cycle oscillations (LCOs), partial amplitude death in oscillator A (PAD$_A$), partial amplitude death in oscillator B (PAD$_B$), and amplitude death (AD) are depicted in the plots.
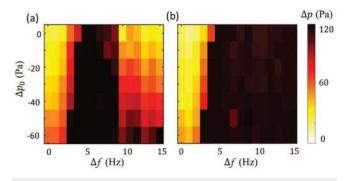
FIG. 6. Two-parameter bifurcation plots showing the effect of variation in amplitude mismatch, Δp_0 and frequency detuning, Δf between the Rijke tube oscillators (a) A and (b) B on their oscillation quenching behavior (Δp). The values of L and D are fixed at 0.48 and 1.0 cm, respectively.

parameters (Δp_0, Δf) indicates the occurrence of LCO in both the oscillators whereas that of $\Delta p \approx 120$ Pa indicates the AD state. The coexistence of Δp near 120 Pa in one of the oscillators and near 0 Pa in another oscillator at a particular value of $\{\Delta p_0, \Delta f\}$ indicates the presence of PAD in the system of coupled oscillators.

From Fig. 4, we see that when the oscillators are coupled with a nearly zero amplitude mismatch ($\Delta p_0 \approx 0$ Pa), coupled dynamics of the oscillators transition from a state of LCO ($\Delta f < 5.0$ Hz) to AD (5.0 Hz $\leq \Delta f \leq 8.0$ Hz) and then to PAD ($\Delta f > 8.0$ Hz) as the frequency detuning in the system is increased. With an increase in the amplitude mismatch in the system, we observe an expansion in the parameter region over which AD is observed. We observe that for values of $|\Delta p_0| > 50$ Pa, the state of amplitude death, which is marked by values of $\Delta p \approx 120$ Pa in both Figs. 6(a) and 6(b), expands to $\Delta f \approx 3.0$ Hz to $\Delta f \approx 15.0$ Hz. From these observations, we conclude that a finite frequency detuning is necessary for the complete quenching of large amplitude LCO, and the addition of mismatch in amplitude and frequency of oscillators facilitates easier suppression of their oscillations.

IV. DISCUSSION

In Secs. III A–III C, we explored the effect of the different system as well as coupling parameters on the amplitude suppression behavior of limit cycle oscillations developed in a pair of coupled prototypical thermoacoustic oscillators. With the use of a single connecting tube of appropriate length and diameter, we showed that limit cycle oscillations having low amplitudes can be completely quenched in both the oscillators. However, in order to quench the limit cycle oscillations with high amplitude in either one or both the oscillators, we need to have a finite frequency detuning in the system. Finally, we demonstrate that the simultaneous presence of amplitude mismatch and frequency detuning enhances the oscillation quenching behavior of coupled thermoacoustic systems.

We notice that the use of the connecting tube induces an acoustic time delay (τ) in the coupling between the thermoacoustic oscillators, as a finite value of time is required for the propagation of

acoustic waves from one oscillator to another. This value of the time delay is proportional to L (i.e., $\propto L'/c$). On the other hand, varying the diameter of the connecting tube results in the variation in its admittance, i.e., $Y = S/\rho c$, where $S = \pi D^2/4$ is the area of cross section of the tube and ρ is the density of ambient air. Thus, depending on the value of D, the amount of acoustic energy transmitted to or reflected from the connecting tube at the junctions of each oscillator (A and B) varies. This, in turn, indicates that the variation in D indirectly controls the strength of coupling between the oscillators.

We observe that, when oscillators of nearly equal amplitude and frequency are coupled, we observe the coexistence of amplitude death (AD) and phase-flip bifurcation (PFB) in the system. In coupled identical oscillators, the dynamics of low amplitude limit cycle oscillations transition from antiphase to in-phase state of synchronization via an intermediate state of AD. However, for high amplitude oscillations, the system displays PFB. Hence, we conjecture that the amplitude of limit cycle oscillations in identical oscillators determines the coupling requisites (length and diameter of the tube) necessary for affecting the amplitude of each oscillator. For a given length and diameter of the connecting tube, when the amplitude of limit cycles is low, the oscillators are weak, and hence the coupling induced due to a given tube diameter is sufficient to cause AD in the system. On the other hand, when the amplitude of limit cycles is sufficiently large, the oscillators are considerably strong that AD is not achievable with the same diameter of the tube, as seen in Fig. 2. Nevertheless, a significant suppression was observed at a critical value of L' corresponding to $L'_{cr} = 112.0$ cm (nondimensionalized as 0.53) for high amplitude oscillations as well. Since the value of L'_{cr} is nearly equal to the length of the Rijke tubes (i.e., $L'_{cr} \approx \lambda/2$), the connecting tube facilitates the propagation of half wave between the oscillators. Here, we note that the limit cycle oscillations are developed in both the systems at the fundamental mode of acoustic oscillations and the boundary conditions of the Rijke tubes correspond to acoustic pressure fluctuations $p' = 0$ Pa at both the ends. Such a propagation of an acoustic half wave from one oscillator to another induces a phase delay (ϕ) of π radians between the signals of coupled oscillators, which can be understood from the following equations.

The phase delay in the propagation of acoustic waves via the connecting tube is given by $\phi = \omega\tau$, where ω is the angular frequency of acoustic waves in the Rijke tube oscillator given by $\omega = 2\pi c/\lambda$ and τ is the time taken by the acoustic wave to propagate via the connecting tube ($\tau = L'/c$) from one oscillator to another. Hence, the phase delay between the two oscillators is given by

$$\phi = \omega\tau = 2\pi \frac{c}{\lambda} \frac{L'}{c} = 2\pi \frac{L'}{\lambda}. \tag{3}$$

When $L' = L'_{cr} = \lambda/2$, we obtain a phase delay of

$$\phi = 2\pi \frac{L'}{\lambda} = 2\pi \frac{\lambda/2}{\lambda} = \pi. \tag{4}$$

This implies that when $L' > L'_{cr}$, the switching of the mean phase difference between the oscillators occurs from $180°$ (antiphase, observed for $L' < L'_{cr}$) to $0°$ (in-phase). We also notice that the maximum suppression is observed in the system for larger connecting

tube diameters (i.e., $D_{cr} \approx 1.0$ cm), indicating a stronger coupling between the oscillators, which is nearly 1/10th of the hydraulic diameter of the Rijke tube oscillator[39] ($D_{hydraulic} = 10.7$ cm, where $D_{hydraulic} = \sqrt{4A/\pi}$ is calculated from the cross-sectional area, A, of the Rijke tube).

Further, we observe that an introduction of frequency detuning near $L' \approx \lambda/2$ induces the phenomenon of AD in the system at low values of detuning and partial amplitude death (PAD) at higher values of detuning. For lower values of detuning, as the wavelength corresponding to the standing wave in both the oscillators is nearly equal, the length of the connecting tube facilitating a phase delay of π [$L' = \lambda/2$ from Eq. (4)] would be near $L \approx 0.5$. Hence, we observe complete suppression of oscillations in both the systems. As the value of frequency detuning is increased, the frequency of oscillator B is higher than that of oscillator A ($f_{0B} > f_{0A}$). This, in turn, suggests that the wavelength and, therefore, the corresponding length of the connecting tube facilitating a phase delay of π belonging to oscillator A is higher than that of oscillator B ($\lambda_{0B} < \lambda_{0A} \Rightarrow L'_B < L'_A$). Hence, as the length of the connecting tube is increased, the occurrence of PAD_B precedes the occurrence of PAD_A. The intermediate lengths of the coupling which would facilitate the phase delay of near π would also lead to the exhibition of AD in the system. Hence, the state of AD is intermediate to the state of PAD_B and PAD_A.

Thus, our study suggests that the optimum length of the connecting tube required to quench the limit cycle oscillations in coupled thermoacoustic systems should be nearly equal to half the wavelength of the acoustic standing wave developed in the system and the optimum diameter should be nearly 1/10th of the system diameter. Our study finds applications in controlling and suppressing undesirable thermoacoustic oscillations produced in various physical systems such as multiple can and can-annular combustors. Moreover, the systematic investigation of oscillation quenching behavior of coupled highly turbulent combustors and systems that exhibit thermoacoustic instabilities with several natural frequencies requires further investigation.

REFERENCES

[1] C. Huygens and H. Oscillatorium, *The Pendulum Clock* (Trans RJ Blackwell, The Iowa State University Press, Ames, 1986).
[2] W. Milsom, "Intermittent breathing in vertebrates," Annu. Rev. Physiol. **53**, 87–105 (1991).
[3] M. E. McIntyre, R. T. Schumacher, and J. Woodhouse, "On the oscillations of musical instruments," J. Acoust. Soc. Am. **74**, 1325–1345 (1983).
[4] T. Yoshida, L. E. Jones, S. P. Ellner, G. F. Fussmann, and N. G. Hairston, Jr., "Rapid evolution drives ecological dynamics in a predator–prey system," Nature **424**, 303 (2003).
[5] C. Duncan, S. Duncan, and S. Scott, "The dynamics of measles epidemics," Theor. Popul. Biol. **52**, 155–163 (1997).
[6] F. Sorg, S. Xalter, M. Muehlbeyer, B. Gellrich, F. Melzer, and T. Ittner, "Oscillation damping system," U.S. patent 6,700,715 (2 March 2004).

[7] H. Takara, S. Kawanishi, and M. Saruwatari, "Stabilisation of a modelocked Er-doped fibre laser by suppressing the relaxation oscillation frequency component," Electron. Lett. **31**, 292–293 (1995).
[8] W. E. Singhose, N. C. Singer, S. J. Derezinski III, B. W. Rappole, and K. Pasch, "Method and apparatus for minimizing unwanted dynamics in a physical system," U.S. patent 5,638,267 (10 June 1997).
[9] C. Ucke and H.-J. Schlichting, "Oscillating dolls and skyscrapers" **39**(3), 139–142 (2008).
[10] M. Oğuztöreli and R. Stein, "The effects of multiple reflex pathways on the oscillations in neuro-muscular systems," J. Math. Biol. **3**, 87–101 (1976).
[11] D. Green and W. G. Unruh, "The failure of the tacoma bridge: A physical model," Am. J. Phys. **74**, 706–716 (2006).
[12] S. H. Strogatz, D. M. Abrams, A. McRobie, B. Eckhardt, and E. Ott, "Theoretical mechanics: Crowd synchrony on the millennium bridge," Nature **438**, 43 (2005).
[13] F. Culick and P. Kuentzmann, Unsteady motions in combustion chambers for propulsion systems, Tech. Rep. (NATO Research and Technology Organization, Neuilly-Sur-Seine, France, 2006).
[14] M. P. Juniper and R. Sujith, "Sensitivity and nonlinearity of thermoacoustic oscillations," Annu. Rev. Fluid Mech. **50**, 661–689 (2018).
[15] T. C. Lieuwen, *Unsteady Combustor Physics* (Cambridge University Press, 2012).
[16] R. Sujith, M. Juniper, and P. Schmid, "Non-normality and nonlinearity in thermoacoustic instabilities," Int. J. Spray Combust. Dyn. **8**, 119–146 (2016).
[17] A. A. Putnam, *Combustion-Driven Oscillations in Industry* (Elsevier Publishing Company, 1971).
[18] A. Bicen, D. Tse, and J. Whitelaw, "Flow and combustion characteristics of an annular combustor," Combust. Flame **72**, 175–192 (1988).
[19] N. A. Kablar, T. Hayakawa, and W. M. Haddad, "Adaptive control for thermoacoustic combustion instabilities," in *Proceedings of the 2001 American Control Conference* (IEEE, 2001), Vol. 3, pp. 2468–2473.
[20] A. Pikovsky, M. Rosenblum, J. Kurths, and J. Kurths, *Synchronization: A Universal Concept in Nonlinear Sciences* (Cambridge University Press, 2003), Vol. 12.
[21] A. Balanov, N. Janson, D. Postnov, and O. Sosnovtseva, *Synchronization: From Simple to Complex* (Springer Science & Business Media, 2008).
[22] Y. Guan, M. Murugesan, and L. K. Li, "Strange nonchaotic and chaotic attractors in a self-excited thermoacoustic oscillator subjected to external periodic forcing," Chaos **28**, 093109 (2018).
[23] S. Mondal, S. A. Pawar, and R. I. Sujith, "Synchronization transition in a thermoacoustic system: Temporal and spatiotemporal analyses," in *Energy for Propulsion* (Springer, 2018), pp. 125–150.
[24] T. Biwa, S. Tozuka, and T. Yazaki, "Amplitude death in coupled thermoacoustic oscillators," Phys. Rev. Appl. **3**, 034006 (2015).
[25] N. Thomas, S. Mondal, S. A. Pawar, and R. I. Sujith, "Effect of time-delay and dissipative coupling on amplitude death in coupled thermoacoustic oscillators," Chaos **28**, 033119 (2018).
[26] H. Jegal, K. Moon, J. Gu, L. K. Li, and K. T. Kim, "Mutual synchronization of two lean-premixed gas turbine combustors: Phase locking and amplitude death," Combust. Flame **206**, 424–437 (2019).
[27] M. Lakshmanan and D. V. Senthilkumar, *Dynamics of Nonlinear Time-Delay Systems* (Springer Science & Business Media, 2011).
[28] J. W. Strutt and B. Rayleigh, *The Theory of Sound* (Dover, 1945).
[29] F. M. Atay, "Total and partial amplitude death in networks of diffusively coupled oscillators," Physica D **183**, 1–18 (2003).
[30] G. W. Swift, "Thermoacoustic engines," J. Acoust. Soc. Am. **84**, 1145–1180 (1988).
[31] N. Thomas, S. Mondal, S. A. Pawar, and R. I. Sujith, "Effect of noise amplification during the transition to amplitude death in coupled thermoacoustic oscillators," Chaos **28**, 093116 (2018).
[32] H. Hyodo and T. Biwa, "Stabilization of thermoacoustic oscillators by delay coupling," Phys. Rev. E **98**, 052223 (2018).
[33] K. I. Matveev, "Thermoacoustic instabilities in the Rijke tube: Experiments and modeling," Ph.D. thesis (California Institute of Technology, 2003).
[34] E. Gopalakrishnan and R. Sujith, "Influence of system parameters on the hysteresis characteristics of a horizontal rijke tube," Int. J. Spray Combust. Dyn. **6**, 293–316 (2014).
[35] A. Koseska, E. Volkov, and J. Kurths, "Oscillation quenching mechanisms: Amplitude vs. oscillation death," Phys. Rep. **531**, 173–199 (2013).

[36]A. Prasad, J. Kurths, S. K. Dana, and R. Ramaswamy, "Phase-flip bifurcation induced by time delay," Phys. Rev. E **74**, 035204 (2006).

[37]K. Manoj, S. A. Pawar, and R. I. Sujith, "Experimental evidence of amplitude death and phase-flip bifurcation between in-phase and anti-phase synchronization," Sci. Rep. **8**, 11626 (2018).

[38]J. Yang, "Transitions to amplitude death in a regular array of nonlinear oscillators," Phys. Rev. E **76**, 016204 (2007).

[39]P. Spoor and G. Swift, "Mode-locking of acoustic resonators and its application to vibration cancellation in acoustic heat engines," J. Acoust. Soc. Am. **106**, 1353–1362 (1999).